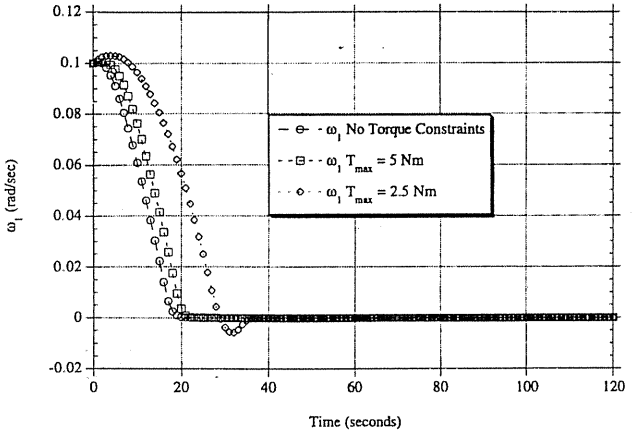

Fig. 1 Angular velocity about e_1 vs time.

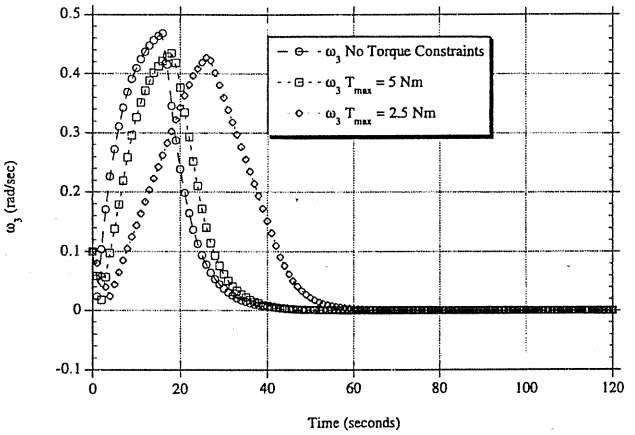

Fig. 2 Angular velocity about e_3 vs time.

the angular velocity about axis 3. A similar statement is true for the angular velocity about e_2, although a figure is not included for succinctness.

Conclusions

Underactuated spacecraft can be detumbled using a variable structure controller. The algorithm converges to a sliding surface on which exponential decay of the angular velocities occurs. Lower maximum torque magnitudes results in slower convergence to the sliding surface. Once the spacecraft is at rest, a series of at most three rotations about the two active axes is used to reorient the spacecraft. Simple linear controllers can be used for the reorientation maneuvers.

References

[1]Coverstone-Carroll, V., and Wilkey, N. M., "Optimal Control of a Satellite-Robot System Using Direct Collocation with Nonlinear Programming," *Acta Astronautica*, Vol. 36, No. 3, 1995, pp. 149–162.

[2]Mukherjee, R., and Chen, D., "Control of Free-Flying Underactuated Space Manipulators to Equilibrium Manifolds," *IEEE Transactions on Robotics and Automation*, Vol. 9, No. 5, 1993, pp. 561–569.

[3]Byrnes, C., and Isidori, A., "On the Attitude Stabilization of Rigid Spacecraft," *Automatica*, Vol. 27, No. 1, 1991, pp. 87–95.

[4]Krishnan, H., Reyhanoglu, M., and McClamroch, H., "Attitude Stabilization of a Rigid Spacecraft Using Two Control Torques: A Nonlinear Control Approach Based on the Spacecraft Attitude Dynamics," *Automatica*, Vol. 30, No. 6, 1994, pp. 1023–1027.

[5]Krishnan, H., McClamroch, N., and Reyhanoglu, M., "Attitude Stabilization of a Rigid Spacecraft Using Two Momentum Wheel Actuators," *Journal of Guidance, Control, and Dynamics*, Vol. 18, No. 2, 1995, pp. 256–263.

[6]Tsiotras, P., and Longuski, J. M., "On Attitude Stabilization of Symmetric Spacecraft with Two Control Torques," *Proceedings of the American Control Conference*, Vol. 1, American Automatic Control Council, San Francisco, CA, 1993, pp. 46–50.

[7]Kaplan, M., *Modern Spacecraft Dynamics and Control*, Wiley, New York, 1976, p. 50.

[8]Slotine, J.-J. E., and Li, W., *Applied Nonlinear Control*, Prentice–Hall, Englewood Cliffs, NJ, 1991, Chap. 7.

[9]Shuster, M., "A Survey of Attitude Representations," *Journal of the Astronautical Sciences*, Vol. 41, No. 4, 1993, pp. 439–517.

Modeling of the Planar Motion of a Flexible Structure

Michael S. Holmes,* A. Ray,† and David R. Mudgett‡
Pennsylvania State University,
University Park, Pennsylvania 16802-1412

Introduction

SLEWING and vibration control of flexible structures have received a considerable amount of attention in recent years. A common control objective is to translate and/or rotate a structure from an initial position to a more desirable final position. Unfortunately, since the structure is flexible, any movement will induce vibration. Thus, the control action should also attempt to suppress any vibrations.

One example of flexible structure control is the fine pointing of a space structure. Vibrations will cause error in the fine pointing and, if severe enough, could even damage the structure. Lim and Balas[1] investigate the fine pointing performance of the controls–structures interaction evolutionary model, which is a laboratory model of a large flexible spacecraft assembled at NASA Langley Research Center. They consider structured and unstructured modeling uncertainties and use μ synthesis to obtain a robust controller.[2]

The objective of the research reported here is to support the planning and fabrication of an experimental facility to study the dynamics of a flexible structure. This involves proposing and modeling the plant, performing computer simulations on the model, and finally building the structure in the laboratory. The ultimate goal is to synthesize a robust control law for the slewing maneuver of the flexible structure. The contribution of this Engineering Note is the derivation of a nonlinear, small-order model for a two-dimensional flexible structure.

Modeling of the Flexible Structure

Figure 1 shows the configuration of the laboratory flexible structure, which was originally proposed by Lim.[3] This structure consists of a rigid body, which undergoes frictionless planar motion in the reference X frame. The center of mass (denoted c.m. in Fig. 1) of the rigid body relative to the X frame is represented by the time-dependent variables $x_1(t)$ and $x_2(t)$. The χ frame of the rigid body has a time-dependent angular orientation $\theta(t)$ with respect to the X frame. A slender flexible beam is connected to the rigid body via a torsional spring at the point (0, c) in the rigid body's χ frame. The beam is free to vibrate only in the plane of the X frame so that the system as a whole can be treated as a two-dimensional problem. The deflection of the flexible beam is expressed in terms of its own local coordinates of the ζ frame. When the flexible beam is undeformed in the equilibrium position, it lies along the ζ_1 axis. Since the beam is rigidly connected to the top end of the spring and the shape of the beam is expressed by a smooth function of the local (ζ frame) coordinates, both the displacement and the slope of the beam are zero at the origin of the ζ frame. As the spring twists, the beam's ζ frame is rotated by an angle of $\phi(t)$ with respect to the rigid body's χ frame.

Received Dec. 13, 1994; revision received Dec. 14, 1995; accepted for publication Dec. 14, 1995.

*Graduate Student, Department of Electrical Engineering.

†Professor, Department of Mechanical Engineering. Associate Fellow AIAA.

‡Assistant Professor, Department of Electrical Engineering.

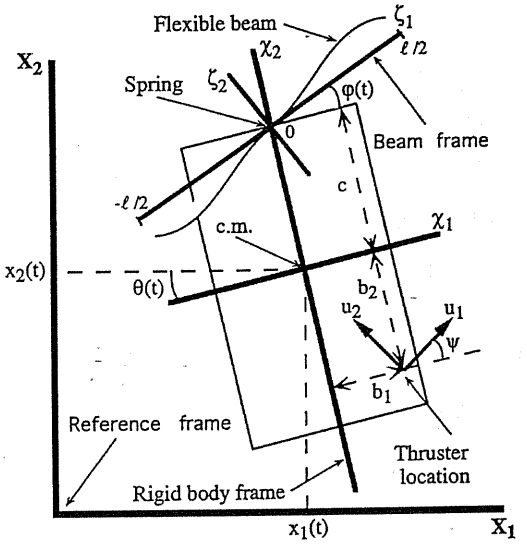

Fig. 1 Schematic diagram of the flexible structure.

There are a total of three torque wheel actuators clamped to the beam whose mass is lumped at points $-\ell/2$, 0, and $\ell/2$ on the ζ_1 axis. The purpose of these actuators is to damp out unwanted beam vibrations. There are also two thrusters connected at point (b_1, b_2) on the rigid body with respect to the χ frame. These thrusters are oriented at a constant angle of ψ and are used to move the structure within the X frame. A total of five sensors are located at points $-\ell/2$, $-\ell/4$, 0, $\ell/4$, and $\ell/2$ on the ζ_1 axis. Thus, the plant will be modeled with five accelerometer sensor outputs and five control inputs. If the plant model is found to be unobservable or poorly observable, however, additional sensors on the rigid body will be required. The following assumptions are made in the modeling of the plant:

1) The deflection of the flexible beam is assumed to be small, which implies that the beam deformation is elastic (i.e., the Young's modulus is constant) and the ζ_1 coordinate of the beam ends remain constant at $z = \pm\ell/2$.

2) The sensors are represented as point masses on the beam, i.e., the moment of inertia of each sensor is negligible.

3) One-half of the spring's mass and moment of inertia is lumped with the rigid body and the other half with the center node of the flexible beam.

4) The cross-sectional dimensions of the flexible beam are small relative to its length. Therefore, both the shear and rotary inertia effects of the beam cross section are neglected.[4] In essence, the flexible beam follows the Euler–Bernoulli equation.

The rigid body modes of the plant are denoted as $q_1 = x_1, q_2 = x_2$ $q_3 = \theta$, $q_4 = \varphi$, $q_5 = \nu_1$, $q_6 = \nu_2$, and $q_7 = \nu_3$, where x_1, x_2, θ, and φ were discussed previously, and ν_1, ν_2, and ν_3 are the relative angular positions of the actuator rotors with respect to the stators (clamped on the flexible beam) at points $z = -\ell/2$, $z = 0$, and $z = \ell/2$, on the ζ_1 axis, respectively.

The bending modes of the flexible beam are represented using the theory of finite elements. The beam is divided into four evenly spaced elements resulting in five nodes. Since the flexible beam is attached to the rigid body with the torsional spring, the beam has zero displacement and slope with respect to the ζ frame at the center node. Thus, there are no states associated with the center node. The plant states $q_8 - q_{15}$ represent the displacement and slope of the beam at the nodes. The amount of displacement of the beam at location z on the ζ_1 axis is approximated as

$$y(z, t) \approx \sum_{j=1}^{8} \Phi_j(z) q_{j+7}(t) \tag{1}$$

where the $\Phi_j(z)$ are constructed using Hermite shape functions.

The kinetic energy of each part of the system needs to be computed. This includes the translation and rotation of the rigid body, the kinetic energy associated with the flexible beam, and the rotation and translation of various lumped masses on the beam.

The kinetic energy (KE) of the rigid body is

$$\mathrm{KE}_{\mathrm{rigid}} = (m_R/2)\left(\dot{x}_1^2 + \dot{x}_2^2\right) + (I_R/2)\dot{\theta}^2 \tag{2}$$

where m_R is the mass of the rigid body including the mass of the thrusters, sensors, half of the spring mass, and any other connected accessories. I_R is the mass moment of inertia about the rigid body's center of mass.

The KE of the flexible beam is

$$\mathrm{KE}_{\mathrm{flex.beam}} = \frac{\rho}{2} \int_{-\ell/2}^{\ell/2} \dot{p}(z, q)^T \, \dot{p}(z, q) \, \mathrm{d}z \tag{3}$$

where ρ is the mass density of the beam (mass/unit length) and $p(z, q)$ represents the location of a point on the deformed beam with respect to the X frame.

Next consider the translational KE of the masses attached to the flexible beam. These masses will be lumped at the five nodes: sensors and actuators at $z = -\ell/2$ and $z = \ell/2$, sensors only at $z = -\ell/4$ and $z = \ell/4$, and a sensor, an actuator, and half of the spring's mass at $z = 0$. Let $z_1 = -\ell/2$, $z_2 = -\ell/4$, $z_3 = 0$, $z_4 = \ell/4$, and $z_5 = \ell/2$. Also let m_i be the total mass lumped at point z_i. Then

$$\mathrm{KE}_{\mathrm{mass\ trans.}} = \frac{1}{2} \sum_{i=1}^{5} m_i \, \dot{p}(z_i, q)^T \, \dot{p}(z_i, q) \tag{4}$$

The rotational KE of the actuator stators and the portion of the spring lumped at the center beam node is determined as follows. The beam's actuators are located at points $z_1 = -\ell/2$, $z_2 = 0$, and $z_3 = \ell/2$. Also, half of the spring's mass is lumped at $z = 0$. It is assumed that the moment of inertia of the sensors is negligibly small. The KE of the stator and spring rotation is

$$\mathrm{KE}_{\mathrm{mass\ rot.}} = \frac{1}{2} \sum_{j=1}^{3} I_{m_j} \left[\dot{\theta} + \dot{\varphi} + \frac{\mathrm{d}}{\mathrm{d}t} \left(\frac{\partial y}{\partial z}\bigg|_{z=z_j} \right) \right]^2 \tag{5}$$

where

$$\frac{\partial y}{\partial z} = \sum_{i=1}^{8} \Phi_i'(z) q_{i+7}(t) \Rightarrow \frac{\mathrm{d}}{\mathrm{d}t} \left(\frac{\partial y}{\partial z} \right) = \sum_{i=1}^{8} \Phi'(z) \dot{q}_{i+7} \tag{6}$$

I_{m_1} and I_{m_3} are the moments of inertia of the stators at points z_1 and z_3 and I_{m_2} is the moment of inertia of the stator at point $z = 0$ plus half of the spring's moment of inertia. Note that

$$\frac{\partial y}{\partial z}\bigg|_{z=0} = 0$$

since the slope of the beam is zero at $z = 0$.

The actuator rotor rotational KE is derived as follows. The beam's actuators are located at points $z_1 = -\ell/2$, $z_2 = 0$, and $z_3 = \ell/2$. The KE of the actuator rotors is

$$\mathrm{KE}_{\mathrm{rotor\ rot.}} = \frac{1}{2} \sum_{j=1}^{3} I_{r_j} \left[\dot{\theta} + \dot{\varphi} + \frac{\mathrm{d}}{\mathrm{d}t} \left(\frac{\partial y}{\partial z}\bigg|_{z=z_j} \right) + \dot{\nu}_j \right]^2 \tag{7}$$

where I_{r_j} is the moment of inertia of the rotor at z_j and ν_j is the angular position of rotor j relative to stator j.

The potential energy (PE) of each part of the system will be computed next. This includes the PE stored in the flexible beam and the torsional spring.

The flexible beam has PE

$$\mathrm{PE}_{\mathrm{beam}} = \frac{EI}{2} \int_{-\ell/2}^{\ell/2} \left[\frac{\partial^2 y(z, t)}{\partial z^2} \right]^2 \mathrm{d}z$$

$$= \frac{EI}{2} \int_{-\ell/2}^{\ell/2} \left[\sum_{j=1}^{2N-2} \Phi_j''(z) q_{j+7}(t) \right]^2 \mathrm{d}z \tag{8}$$

where E is the elasticity of the beam and I is the area moment of inertia.

The torsional spring connecting the flexible beam to the rigid body has PE

$$\mathrm{PE}_{\mathrm{spring}} = \tfrac{1}{2} K_{\mathrm{spring}} \varphi^2 \tag{9}$$

where K_{spring} is the spring constant.

It is possible to write the total kinetic and potential energy of the plant in the form

$$\mathrm{KE}_{\mathrm{total}} = \tfrac{1}{2}\dot{q}^T[A_0 + A_1(q) + A_2(q) + A_3 + A_4]\dot{q} \tag{10}$$

$$\mathrm{PE}_{\mathrm{total}} = \tfrac{1}{2} q^T (B_1 + B_2) q \tag{11}$$

The seven energy contributions can be summarized as follows:

A_0 = KE of the rigid body

$A_1(q)$ = KE of the flexible beam

$A_2(q)$ = translational KE of the masses lumped on the beam

A_3 = rotational KE of the actuator stators and the portion of the spring's mass lumped at the center beam node

A_4 = rotational KE of the actuator rotor

B_1 = PE stored in the flexible beam

B_2 = PE stored in the torsional spring

The virtual work done by the thrusters and the torque wheel actuators is now calculated. The thruster inputs u_1 and u_2 are the only forces contributing to the rigid body's virtual work. The virtual work done on the rigid body can be shown to be

$$\begin{aligned}\delta W_{\mathrm{rigid}} &= [u_1 \cos(\theta + \psi) - u_2 \sin(\theta + \psi)]\delta x_1 \\ &+ [u_1 \sin(\theta + \psi) + u_2 \cos(\theta + \psi)]\delta x_2 \\ &+ [b_1(u_1 \sin\psi + u_2 \cos\psi) - b_2(u_2 \sin\psi - u_1 \cos\psi)]\delta\theta\end{aligned} \tag{12}$$

The beam actuators located at $z_1 = -\ell/2$, $z_2 = 0$, and $z_3 = \ell/2$ contribute to the virtual work done on the flexible beam. The actuators provide a torque of u_i at beam position z_i. The virtual work done on the flexible body is

$$\begin{aligned}\delta W_{\mathrm{flex}} = \sum_{j=1}^{3} \Bigg\{ & u_{j+2}\delta\left(\theta + \varphi + \left.\frac{\partial y}{\partial z}\right|_{z=z_j} + v_j\right) \\ & - u_{j+2}\delta\left[+ \left(\theta + \varphi + \left.\frac{\partial y}{\partial z}\right|_{z=z_j}\right)\right]\Bigg\}\end{aligned} \tag{13}$$

where the first term is a result of the angular displacement of the rotors and the second term is a result of the angular displacement of the stators. This can also be written as

$$\delta W_{\mathrm{flex}} = \sum_{j=1}^{3} u_{j+2}\delta v_j \tag{14}$$

The total virtual work done on the system can be expressed as

$$\delta W_{\mathrm{total}} = \sum_{i=1}^{15} Q_i \delta q_i \tag{15}$$

where

$$\begin{aligned} Q_1 &= u_1 \cos(q_3 + \psi) - u_2 \sin(q_3 + \psi) \\ Q_2 &= u_1 \sin(q_3 + \psi) + u_2 \cos(q_3 + \psi) \\ Q_3 &= b_1(u_1 \sin\psi + u_2 \cos\psi) - b_2(u_1 \cos\psi - u_2 \sin\psi) \\ Q_4 &= 0, \qquad Q_{i+4} = u_{i+2}, \qquad i = 1, 2, 3 \\ Q_{i+7} &= 0, \qquad i = 1, 2, \ldots, 8 \end{aligned} \tag{16}$$

The Lagrangian of the system is

$$L = \mathrm{KE}_{\mathrm{total}} - \mathrm{PE}_{\mathrm{total}} \tag{17}$$

or, using $\mathrm{KE}_{\mathrm{total}}$ and $\mathrm{PE}_{\mathrm{total}}$ just derived,

$$L = \tfrac{1}{2}\dot{q}^T[A_0 + A_1(q) + A_2(q) + A_3 + A_4]\dot{q} - \tfrac{1}{2} q^T (B_1 + B_2) q \tag{18}$$

Using the Euler–Lagrange equation

$$\frac{\mathrm{d}}{\mathrm{d}t}\left(\frac{\partial L}{\partial \dot{q}}\right) - \frac{\partial L}{\partial q} = Q \tag{19}$$

yields

$$\begin{aligned}&[A_0 + A_1(q) + A_2(q) + A_3 + A_4]\ddot{q} + \frac{\mathrm{d}}{\mathrm{d}t}[A_1(q) + A_2(q)]\dot{q} \\ &\quad - \frac{1}{2}\frac{\partial}{\partial q}\left\{\dot{q}^T[A_1(q) + A_2(q)]\dot{q}\right\} + (B_1 + B_2)q = Q(q, u)\end{aligned} \tag{20}$$

as the equation of motion, where A_i and B_i are 15×15 matrices and q and Q are 15×1 vectors.

The plant model as given in Eq. (20) contains no damping term. Although the $\mathrm{d}/\mathrm{d}t(\bullet)$ term looks like damping, it comes about because of the nonlinearities in the system and not because of any damping effect. In the actual plant, however, there will be some damping present (e.g., the bending of the flexible beam and the twisting of the torsional spring will produce heat). It is possible to artificially add damping to the plant model. The term $D\dot{q}$ can be added to the left-hand side of Eq. (20), where D is a diagonal matrix which contains positive damping terms for each plant model state. For example, a positive real number in D (4, 4) element will account for the damping resulting from the torsional spring. To obtain matrix D, one must either estimate the damping effects of the plant or determine them experimentally.

It is necessary to reformulate the equations of motion as just developed into a more convenient form to facilitate the writing of an efficient simulation code. This involves finding solutions of the spatial integrations a priori and using algebraic and trigonometric properties to simplify the model equations.[5] A numerically efficient simulation program has been coded based on these considerations. Simulation results for a given set of system parameters are reported elsewhere.[5]

Summary, Conclusions, and Future Work

A 30-state nonlinear model for a two-dimensional flexible structure has been developed and tested by performing computer simulations. The method of Lagrangian mechanics has been used to model the plant. Finite elements methods were used to describe the motion of the Euler–Bernoulli beam contained in the structure.

The modeling of the structure is a necessary first step to finding a robust controller that along with an a priori determined open-loop input sequence will transfer the plant from an initial state to a desired final state.

To verify the validity of the model, the actual flexible structure should be built and tested in the laboratory. Comparisons between laboratory measurements and computer simulation results will indicate the accuracy of the mathematical model. If the model is not sufficiently accurate, it could be very difficult to design a controller that satisfies the robust performance criteria.[6] In such a case the model will need to be refined. For example, a larger number of nodes may be necessary in the finite element formulation. The accuracy of the finite element model of the flexible beam has been examined for a given set of parameters as presented in an earlier report.[5] The finite element description of the beam is the source of 16 out of the 30 states in the plant model if a total of five nodes are selected in the flexible beam model. Increasing the number of finite element nodes from five to a larger number would add four more states for each additional node. Also, to keep the nodes symmetric across the beam (with a node at the center of the beam), additional nodes would need to be added in pairs. Thus, an attempt to improve accuracy by adding more nodes will greatly increase the number of states in the model. Moreover, the addition of more nodes may increase accuracy only marginally. The task of control synthesis requires a tradeoff between the accuracy and complexity of the plant model that should be made based on the parameters of the flexible beam.

The next step in the design process is to determine an open-loop control law. This can be accomplished by minimizing an appropriate cost functional under specified state and control input constraints. A nonlinear programming package (e.g., NPSOL[7]) can be used to generate the optimal time history of the control inputs.

The open-loop control policy, when applied to the actual system, may not produce the desired output because of modeling uncertainties, external disturbances, and a mismatch in the initial conditions. Techniques such as the structured singular value (μ) (Ref. 6) for energy-bounded signals, or ℓ_1 (Ref. 8) for amplitude-bounded persistent signals, can be used to synthesize a robust controller, which will attempt to eliminate these errors.

Acknowledgments

This research was supported in part by NASA Langley Research Center under Grant NAG 1-1417. The authors acknowledge benefits of discussion with Marc Carpino and Kyong B. Lim.

References

[1]Lim, K. B., and Balas, G. J., "Line-of-Sight Control of the CSI Evolutionary Model: μ Control," *Proceedings of the American Control Conference*, Chicago, IL, 1992, pp. 1996–2000.

[2]Packard, A., Doyle, J., and Balas, G., "Linear, Multivariable Robust Control with a μ Perspective," *Transactions of the ASME, Journal of Dynamic Systems, Measurement and Control*, Vol. 115, June 1993, pp. 426–438.

[3]Lim, K. B., "A Unified Approach to Structure and Controller Design Optimizations," Ph.D. Dissertation, Dept. of Aerospace Engineering, Virginia Polytechnic Inst. and State Univ., Blacksburg, VA, 1986.

[4]Timoshenko, S., *Vibration Problems in Engineering*, 3rd ed., Van Nostrand, Princeton, NJ, 1955, pp. 341, 342.

[5]Holmes, M. S., "Modeling of the Planar Motion of a Proposed Laboratory Flexible Structure," M.S. Thesis, Dept. of Electrical Engineering, Pennsylvania State Univ., State College, PA, 1994.

[6]Balas, G. J., and Doyle, J. C., "Robustness and Performance Tradeoffs in Control Design for Flexible Structures," *Proceedings of the 29th IEEE Conference on Decision and Control*, Honolulu, HI, 1990, pp. 2999–3010.

[7]Gill, P. E., Murray, W., Saunders, M. A., and Wright, M. H., "User's Guide for NPSOL (Version 4.0): A Fortran Package for Nonlinear Programming," Office of Technology Licensing, Palo Alto, CA, Jan. 1986.

[8]Dahleh, M. A., and Diaz-Bobillo, I. J., *Control of Uncertain Systems*, Prentice–Hall, Englewood Cliffs, NJ, 1995.

Self-Sensing Magnetostrictive Actuator for Vibration Suppression

Lowell Dale Jones* and Ephrahim Garcia†
Vanderbilt University, Nashville, Tennessee 37235

Nomenclature

A	= area
B	= flux density
$\hat{d}, \hat{e}$	= piezomagnetic constants
H	= magnetic field
i	= current
L	= inductance
ℓ	= length
n	= number of wire turns
R	= resistance
S, ε	= strain
s	= elastic compliance
T, σ	= stress
v	= voltage
Y	= elastic stiffness
μ	= permeability
Φ	= magnetic flux

Received Sept. 28, 1994; revision received Nov. 28, 1995; accepted for publication Jan. 30, 1996.

*Graduate Assistant, Smart Structures Laboratory, Department of Mechanical Engineering.

†Associate Professor, Smart Structures Laboratory, Department of Mechanical Engineering. Member AIAA.

Introduction

THE concept of a self-sensing actuator originated in the control of electromagnetic mechanisms used in ordinary speakers.[1] The technique was proposed as a simple method for adding damping to their resonant modes. By using simple bridge circuitry, a signal could be generated independent of the applied control voltage that is proportional, albeit with some frequency dependence, to the velocity of the coil being driven in the magnetic field.

Recent work has applied the self-sensing concept to the control of smart materials, specifically piezoceramics and magnetostrictives.[2–7] Pratt and Flatau[6] first investigated the concept of a self-sensing magnetostrictive actuator. A self-sensing model was proposed as was an initial investigation into the use of a magnetostrictive actuator for active isolation. The experiments were limited in their success because of the high bandwidth the actuator system was trying to control. Fenn and Gerver[7] also developed models and produced data, which supported the use of magnetostrictive materials in a self-sensing configuration. The success of applying the self-sensing technique to a magnetostrictive active strut as it is presented in this Note is largely due to focusing on the damping of low-frequency modes of a truss structure.

Magnetostriction Overview

Even though magnetostriction, like electrostriction, is inherently a second-order effect, it is common to treat it as a problem in linear elasticity using the approximation of small strain theory.[8,9] Treating the effects in this fashion results in a one-to-one analogy to the constitutive relations defining linear piezoelectricity theory.[9,10] Thus, a practical form of the magnetostrictive constitutive relations is expressed as follows:

$$S_{ij} = s^H_{ijkl} T_{kl} + \hat{d}_{kij} H_k \tag{1}$$

$$B_i = \hat{e}_{ikl} S_{kl} + \mu^S_{ik} H_k \tag{2}$$

This form is more practical because of its ease of use in approximation methods.

Since we are only concerned with a one-dimensional case where the stress, strain, and fields are applied/measured in the same direction and the magnetostrictive material is assumed to be isotropic, these tensor equations can be compressed into the following set:

$$\varepsilon = (\sigma/Y) + \hat{d}H \tag{3}$$

$$B = \hat{e}\varepsilon + \mu H \tag{4}$$

For experimentation, it is helpful to further manipulate Eqs. (3) and (4) to gain some intuition for the problem as well as simplifying the simulation process. Using a priori knowledge of the active magnetostrictive element, i.e., the actuator, some simplifying assumptions can be made. The actuator can be modeled as a simple wire-wound solenoid assuming the wires are thin, the spacing between the wires is small relative to the solenoid's radius, the solenoid is long relative to its diameter, and the magnetostrictive material enclosed has a constant permeability. The field induced by current flow in a simple solenoid is given as

$$H = (n/\ell)i \tag{5}$$

When Eq. (5) is substituted into Eq. (3) the following results:

$$\varepsilon = (\sigma/Y) + \hat{d}(n/\ell)i \tag{6}$$

Equation (6) shows the strain to be clearly a result of two effects, one of an imposed stress and an imposed current through the wire.

Turning now to Eq. (4), we can use fundamental laws of magnetics to derive an equation in terms of voltage and current instead